

Electrical characterisation of stearic acid/calix[4]amine Langmuir–Blodgett thin film



Rifat Çapan^{a,*}, Tim Richardson^{b,1}, Aseel K. Hassan^c, Frank Davis^d

^a Physics Department, Science and Literature Faculty, Balıkesir University, 10145 Balıkesir, Turkey

^b Physics and Astronomy Department, Sheffield University, Hounsfield Road, Sheffield S3 7HR, UK

^c Computer, Engineering and Science Faculty, Sheffield Hallam University, Sheffield S1 2NU, S Yorkshire, UK

^d Cranfield Health, Cranfield University, Beds MK43 0AL, UK

HIGHLIGHTS

- Stearic acid and calix[4]amine thin film successfully deposited.
- The value of the pyroelectric figure of merit was determined.
- Stearic acid/calix[4]amine LB film showed an ohmic conductivity at low voltages.
- Conductivity obeyed the Schottky conduction mechanism at higher voltages.
- The frequency dependence of conductivity shows a power law relationship.

ARTICLE INFO

Article history:

Received 26 April 2013

Received in revised form

25 September 2013

Accepted 19 October 2013

Keywords:

Thin films

Electrical characterisation

Pyroelectric measurements

Organic compounds

ABSTRACT

Within this work we deposited 16 monolayers of stearic acid alternated with 15 monolayers of calix[4]amine to form a non-centrosymmetric Langmuir–Blodgett (LB) thin film onto an aluminized (50 nm coated) glass microscopic slide. Dielectric constant and dielectric loss for the film were determined using $C-f$ and $\tan(\delta-f)$ measurements. The value of the pyroelectric figure of merit was determined as $1.73 \mu\text{C m}^{-2} \text{K}^{-1}$. To elucidate the conduction mechanism of stearic acid/calix[4]amine LB film, DC current–voltage measurements between -4 and $+4$ V were carried out. The $I(V)$ behaviour shows a symmetrical and highly non-linear behaviour. Analysis of this behaviour of the stearic acid/calix[4]amine LB film showed a conductivity value of $1.12 \times 10^{-13} \text{ S m}^{-1}$ for ohmic region. The exponential part of $I(V)$ dependence obeyed the Schottky conduction mechanism with a barrier height of 1.67 eV. This LB film structure shows a typical insulating behaviour for low voltage values and the Schottky effect becomes dominant when the voltage increases. The frequency dependence of conductivity shows a power law relationship between conductance and frequency.

© 2013 Elsevier B.V. All rights reserved.

1. Introduction

Molecular electronics is an interdisciplinary field of research, encompassing physics, chemistry and materials science. The unifying feature of the area of research is the use of molecular building blocks for the fabrication of electronic and optoelectronic devices using organic, inorganic and hybrid materials. This subject also deals with the manipulation of these materials at the nanometre scale to realize a nano device that will store and/or process information [1]. Organic materials can yield semiconductive and even metallic properties with a high physical and chemical stability, a

wide range of working temperatures, relatively facile processing methods as well as allowing the construction of controlled molecular arrangements. This makes it possible to fabricate devices such as diodes, field effect transistors (FET), organic light emitting displays (OLED), pyroelectric detectors [2,3] as well as biomedical devices [4] and motion detectors [5] using these materials. Organic materials are widely utilised for the construction of pyroelectric devices and similar applications because of their ease of preparation, low dielectric constant and dielectric loss. However they often demonstrate a smaller pyroelectric coefficient than other type of pyro materials. Langmuir–Blodgett (LB) thin film deposition technique is one of the best methods used to manipulate organic materials at the molecular level and to fabricate devices consisting of a layered Metal/LB film/Metal (M/LB/M) structure, suitable for pyroelectric and electronic applications.

* Corresponding author. Tel.: +90 266 6121000; fax: +90 266 6121215.

E-mail address: rcapan@balikesir.edu.tr (R. Çapan).

¹ Deceased.

A number of organic materials have been utilised for pyroelectric measurements such as arachidic acid/1,2-bis(dodecyloxy)-4,5-diaminobenzene alternate layer LB films [6], polysiloxane/eicosylamine LB films with and without KCl and CaCl₂ [7] as well as alternating hemicyanine/nitrogen crown LB films incorporating barium ions [8]. In recent years, calix[*n*]arene derivatives have been extensively studied due to their possible applications for pyroelectric heat sensor materials as well as being highly selective molecular receptors for various metal ions and organic compounds [9]. Several calix[*n*]arene molecules have been synthesised and used to form pyroelectric films. Previous work demonstrated the formation of non-centrosymmetric Z-type calix[4]acid LB films [10], calix[4]acid/amine alternate layer LB films [11], copolysiloxane/calix[8]arene alternate layer LB films [12] and pyroelectric calix[8]arene LB films [13,14]. The main source of pyroelectric effect in LB films is explained by a combination of three main mechanisms; these being proton transfer, tilting and ion interaction mechanisms [15,16]. Another mechanism for pyroelectricity in LB film structures has been proposed as an additional source of the pyroelectric response; this involves the temperature-dependent dipolar tilting in which the alignment of dipolar entities relative to the substrate normal changes as a function of temperature [17,18].

Electrical conduction in molecular materials is strongly dependent on the physical arrangement of molecules in the solid state. The electrical ability of the material to transport electrical charges (the conductivity) or to store charge (the dielectric constant) can be examined using an applied voltage or measuring the capacitance versus frequency [19]. Current flow through an LB film structure as a function of applied voltage according to the relation $\log J \propto V^n$ has been previously described by a combination of two mechanisms: (i) electron tunnelling through each LB bilayer, and (ii) thermally activated hopping within the plane of carboxylic head groups [20]. To identify the conduction processes through 22-tricosenoic acid LB film, the $I(V)$ characteristics of the film were compared with the behaviour expected from a theoretical model of the conduction processes. The Poole–Frenkel (excitation of carriers out of traps in the insulating film) and Schottky (the injection of carriers from the electrodes over the potential barrier formed at the insulator–metal interface) conduction mechanisms were compared with the experimental observations [21,22].

In this study, a hybrid alternate layer LB film of stearic acid which contains a polar carboxyl headgroup, co-deposited with a calix[4]arene molecular basket substituted with primary amine groups is examined for the first time. This LB film structure yields temperature-dependent pyroelectric current and electronic conduction. This article reports the results of pyroelectric measurements, $I(V)$ measurements to determine the DC conduction mechanism as well as measuring AC properties, mainly capacitance measurements over a wide range of frequencies for M/LB/M sandwich structure.

2. Experimental details

2.1. Metal–LB film–Metal device preparation

The chemical structure of materials used is shown in Fig. 1. Alternate layer LB films consisting of 16 monolayers of stearic acid and 15 monolayers of calix[4]amine were prepared using a NIMA 622 type LB trough possessing a central fixed barrier accommodating a rotating drum to which the substrate is attached. Stearic acid and calix[4]amine were spread onto the water surface using a concentration of approximately 1 mg ml⁻¹ and 0.8 mg ml⁻¹ solution in chloroform respectively. A time period of 15 min was allowed for the solvent to evaporate before the area enclosed by the barriers was reduced. The LB film monolayers were sequentially

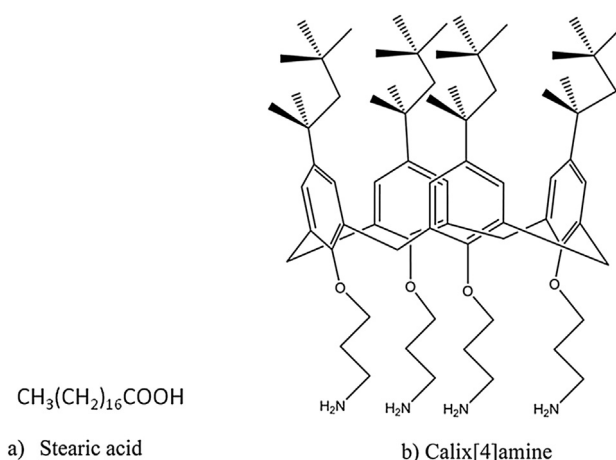


Fig. 1. The chemical structures of the materials.

transferred onto an aluminised glass substrate by the alternate layer LB deposition technique at a surface pressure of 22.5 mN m⁻¹. Stearic acid was deposited on each upstroke with a deposition speed of 10 mm min⁻¹ while calix[4]amine monolayers were deposited on the downstroke of the substrate at a speed of 20 mm min⁻¹.

The substrates used for these LB multilayer assemblies were aluminised (50 nm coating) glass microscopic slides. An Edwards 306A vacuum-evaporator was used for the deposition of aluminium bottom and top electrodes. The bottom electrode of 50 nm was evaporated directly onto a clean glass substrate at a rate between 3 and 6 Å s⁻¹ from a tungsten filament. A shadow mask was used for the deposition of top electrodes, which were evaporated onto the LB films in two stages. In the first stage a slow evaporation rate (approximately 0.01–0.03 nm s⁻¹) for 5 min was used to deposit the top electrode. During the second stage, this rate was increased to 0.5–0.7 nm s⁻¹ until 50 nm has been deposited. The temperature and pressure were kept below 30 °C and 10⁻⁵ torr respectively during the evaporation. The structure of the pyroelectric LB device (Al, Al₂O₃/LB film/Al) used is shown in Fig. 2.

2.2. Electrical measurements

The pyroelectric effect is the temperature-dependent spontaneous electric polarization within a material possessing a non-centrosymmetric structure. The pyroelectric measurement itself was a quasi-static technique in which the pyroelectric sample was heated and cooled by a non-radiative source in a controlled manner allowing a small temperature change (typically ±1 K) using a Peltier heating device. Fig. 2 shows a schematic diagram of the quasi-static pyroelectric measurement system. The M/LB/M device was placed in a special sample chamber, which is electrically earthed. The temperature of LB device was controlled using a 18W Peltier effect heat pump, which was in thermal contact with a copper block on which the LB film device was mounted. Cold water was allowed to circulate through the copper block to help maintain uniform changes of temperature over the area of the LB device. A good thermal contact between LB film device and the copper block was made with a zinc oxide heat sink compound, which has low electrical conductivity and high thermal conductivity.

A welded tip type K (Ni–Cr/Ni–Al) thermocouple was placed at the M/LB/M device surface and connected to a Jenway 7900 thermometer in order to measure the temperature of the LB device. A good electrical contact between the electrodes and the gold

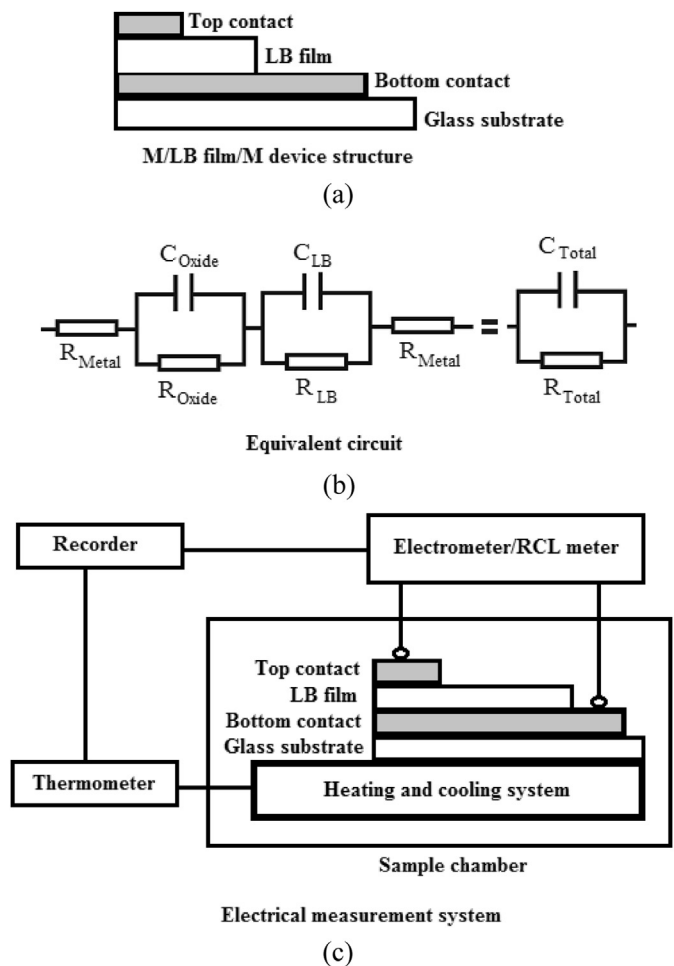


Fig. 2. Device and measurement system a) M/LB/M device structure b) equivalent circuit c) measurement system.

leads was made using silver-loaded conducting paste (RS Components). The chamber was evacuated to $\sim 4\text{--}6$ Pa (10^{-2} torr) using an Edwards E2M5 two-stage rotary vacuum pump. The device was kept under vacuum with short-circuited electrodes for at least 6 h before testing to avoid any thermal current problems due to absorbed moisture and trapped charge collected from the air. The pyroelectric current was measured using a Keithley 614 electrometer and a Jenway 7900 thermometer was connected to one channel of a Scientific Instrument 312 chart recorder. A convenient method of determine the pyroelectric coefficient was to impose a triangular wave temperature profile on the sample by heating or cooling and to measure the resulting square wave current profile generated from the pyroelectric LB sample. Fig. 3a shows the ideal data of the temperature and pyroelectric current profiles which can be used to calculate the pyroelectric coefficient of LB film.

Electrical measurements ($I(V)$, $C(f)$ and $\tan \delta(f)$) were carried out using a Keithley 6517A electrometer and a Hewlett Packard 4284 automatic RCL meter with a microprocessor controlled measuring system. The device was kept under vacuum before testing for the reasons explained above. DC electrical measurements were performed in the range of ± 4 V and AC measurements over a frequency range from 20 Hz to 1 MHz. Both measurements were performed at 22 °C. The dielectric constant and dielectric loss were obtained to determine the figure of merit for this LB film device.

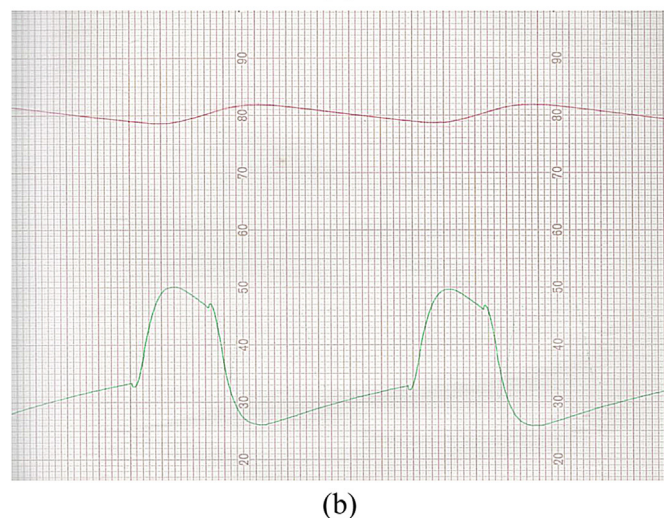
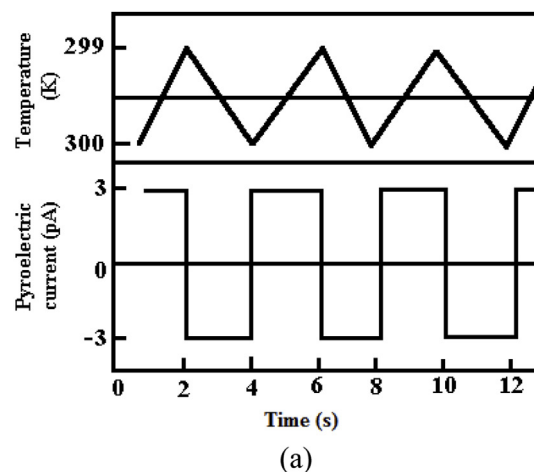


Fig. 3. a) An ideal example of a square-wave form for a triangular temperature profile, b) experimental result of a square-wave form (green colour) for triangular temperature profiles (red colour). (For interpretation of the references to colour in this figure legend, the reader is referred to the web version of this article.)

3. Analysis of results and discussion

3.1. Pyroelectric figure of merit

When the M–LB–M device structure shown in Fig. 2 is subjected to a temperature gradient, a charge is developed across the material in response to the change in electric dipole. This leads to a flow of current (I) when the electrodes of the device are connected together via a sensitive electrometer. It is well known that some LB film materials generate a pyroelectric current when they are heated and cooled. This pyroelectric current, I , is proportional to the rate of change of polarisation with respect to temperature as shown below [17]:

$$I = \Gamma A \frac{dT}{dt} \quad (1)$$

where dT/dt is the rate of temperature change, A is the area of overlap of the two electrodes (4.15×10^{-6} m²) and Γ is the pyroelectric coefficient (the rate of change of polarisation with respect to temperature).

The quasi-static measurement system yields a triangular shaped temperature profile (i.e. demonstrating a uniform temperature

gradient) over the LB film sample, and thus a square-wave (derivative of temperature change) current is observed. A special sample chamber was used to heat and cool the LB film sample while a temperature controller was utilized to generate a triangular shaped temperature profile at 22 °C using the changing rates of 0.056 °C s⁻¹ for heating ramps, 0.028 °C s⁻¹ for cooling ramps. The resultant pyroelectric current was measured using an electrometer (Keithley 614). Both temperature controller and electrometer were connected to a chart recorder for data recording (see Fig. 3b). The amplitude of this square-wave current profile and the magnitude of the temperature gradients are used to determine the pyroelectric coefficient using Eq. (1) which is found to be 0.23 °C m⁻² K⁻¹ at 22 °C. The pyroelectric effect increases with rising temperature due to tilting and proton transfer between carboxylic acid and amine groups [6,16].

The dielectric constant of pyroelectric LB film sample as a function of film thickness can be described as [7]:

$$\epsilon_r = \left(\frac{CNd}{\epsilon_0 A} \right) \quad (2)$$

where C is the capacitance of LB film, N is the layer number, d is the thickness of LB film, ϵ_0 is the permittivity of free space (8.854×10^{-12} F m⁻¹) and A is the effective electrode area.

Fig. 4 shows a plot of the capacitance and dielectric loss against $\log f$ for 31 monolayers of stearic acid/calix[4]amine LB film at 22 °C. The capacitance value gradually decreases with increasing frequency except for the last three points which drops noticeably. A reasonable explanation of the observed decrease in capacitance with increasing frequency may lie in disorientation of amphiphilic molecules and the resulting reduction in the polarisability of alternate layer LB films [23]. Stearic acid/calix[4]amine LB film demonstrate a traditional insulating behaviour and there is no evidence of any Debye type dipolar relaxation.

From Oliviere et al. the molecular thickness of the calix[8]arene acid molecule is found to be 1.5 nm using Corey–Pauling–Koltun (CPK) models [16]. The thickness of stearic acid monolayer is known to be 2.5 nm [24]. The dielectric constant of stearic acid/calix[4]amine LB film is estimated as 2.5.

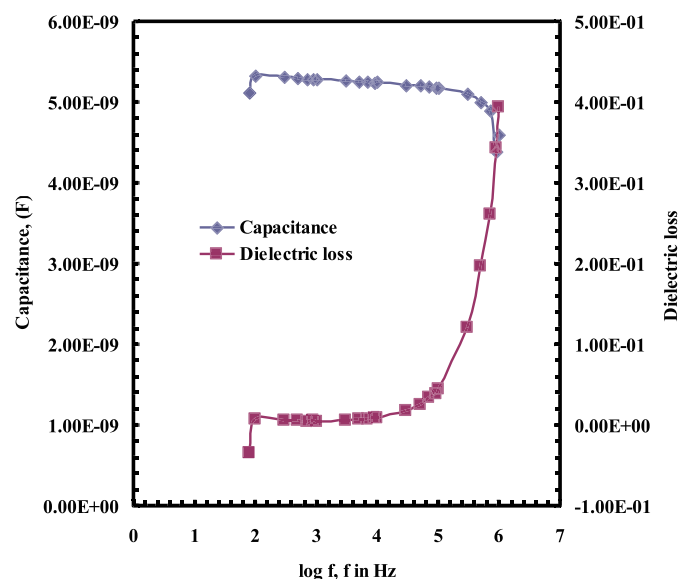


Fig. 4. Plot of the capacitance and dielectric loss against $\log f$.

The Figure of Merit (FOM) is one of the most important parameters for the design of pyroelectric detectors and is described for an LB film by Ref. [8]:

$$\text{FOM} = \frac{\Gamma}{\sqrt{\epsilon_r \tan \delta}} \quad (3)$$

where Γ is the pyroelectric coefficient of LB film, ϵ_r and $\tan \delta$ are the dielectric constant and dielectric loss, respectively. For the best performance of the pyro device, the pyroelectric material must have a high pyroelectric activity, a low dielectric constant and dielectric loss. In this work, a value of FOM at 100 Hz for stearic acid/calix[4]amine is found to be 1.73 °C m⁻² K⁻¹ using Eq. (3). Organic materials usually give low FOM values when they are compared with single crystal or ceramics due to their small pyroelectric coefficients.

3.2. DC measurement analysis

In order to study the conduction mechanism through our LB film structure the form of the $I(V)$ characteristics was compared to the behaviour expected from the theoretical model of the conduction mechanism through Metal–LB film–Metal (M–LB–M) device. The $I(V)$ behaviour is symmetrical and highly non-linear. The data were analysed by a method of decomposition within two conduction regions; these are the linear and exponential dependence regions. Each one of these two regions corresponds to a specific carrier conduction mechanism as described below:

i) Linear (Ohmic) behaviour:

Within the linear portion of the $I(V)$ plot, the current through a M–LB film–M structure is directly proportional to the applied voltage and the conductivity, σ is described by the following relationship:

$$\sigma = \frac{Id}{VA} \quad (4)$$

where d is the film thickness and A is the electrode area.

ii) Exponential behaviour:

The electron transport within the exponential region was analysed using two different mechanisms; these are Poole–Frenkel and Schottky conduction. The dependence of current on voltage due to these different processes was compared with our experimental observations.

The Poole–Frenkel effect describes a bulk limited conduction process due to trap barrier lowering with applied electric field [25,26]. This effect is associated with the excitation of carriers out of traps in the insulating film and the current–voltage dependence is described by Refs. [21,23].

$$J = J_0 \exp\left(\frac{\beta_{\text{PF}} V^{1/2}}{kTd^{1/2}}\right) \quad (5)$$

where J_0 is the low field current density, T is the absolute temperature, k is the Boltzmann's constant, d is the film thickness and β_{PF} is Poole–Frenkel field-lowering coefficients, which is given by Ref. [27]:

$$\beta_{\text{PF}} = \left(\frac{e}{\pi \epsilon_r \epsilon_0} \right)^{1/2} \quad (6)$$

where e is the electron charge, ϵ_r is the dielectric constant of LB films and ϵ_0 is the free space permittivity.

The Schottky conduction mechanism describes the interaction of an electric field at a metal–insulator interface and the image force inducing a lowering of the potential barrier [26]. The injection of carriers from the electrodes over the potential barrier formed at the insulator–metal interface can be described by Ref. [28]:

$$J = AT^2 \exp\left(-\frac{\Phi_S}{kT}\right) \exp\left(\frac{\beta_S V^{1/2}}{kTd^{1/2}}\right) \quad (7)$$

where A is the Richardson constant, Φ_S is the Schottky barrier height at the injecting electrode interface, and the other parameters are as defined above. β_S is the Schottky coefficient, which is given by Ref. [28]:

$$\beta_S = \frac{1}{2} \left(\frac{e}{\pi \epsilon_r \epsilon_0} \right)^{1/2} \quad (8)$$

The difference between these two conduction mechanisms results in a different value for β which can be calculated using the gradient of the $\ln J$ versus $V^{1/2}$ graph. The relationship between two β values is $\beta_{PF} = 2\beta_S$.

Fig. 5 shows the current–voltage characteristic of the stearic acid/calix[4]amine LB film measured through the M/LB film/M device. These characteristics can be thought of as comprised of different regions representing different conduction regimes. Each of these regions corresponds to a specific carrier conduction mechanism. The $I(V)$ plot displays an ohmic behaviour which occurs below 1.2 V followed by a non-ohmic behaviour. The electrical conductivity calculated in the ohmic range is about $1.12 \times 10^{-13} \text{ S m}^{-1}$, a value which is characteristic of an insulator. Between 1.2 and 4 V, the current is linearly proportional to the square root of the applied voltage. This can be explained by the Poole–Frenkel or Schottky effect, which is caused by a potential barrier. This $I(V)$ dependence was analysed by a method of decomposition within two regions.

The linear dependence of $\ln J$ as a function of $V^{1/2}$ in the voltage range of 1.2–2.0 V is given in Fig. 6. The experimental value of β for an LB film can be calculated from the gradient of the $\ln J$ versus $V^{1/2}$ plots. The slope can be described by Refs. [13,29].

$$m = \frac{\beta}{kTd^{1/2}} \quad (9)$$

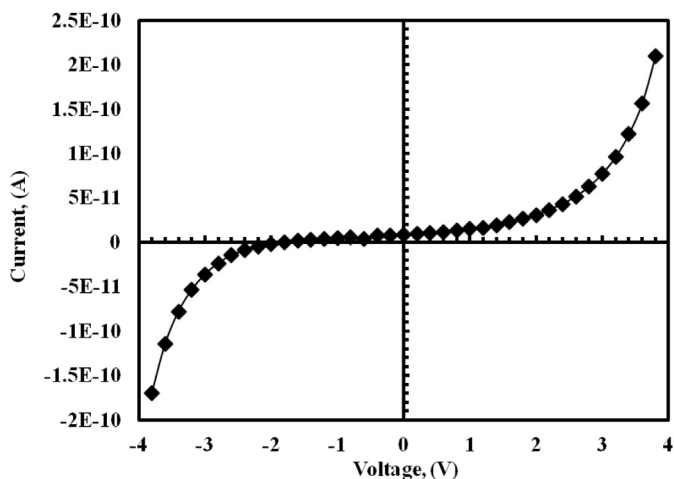


Fig. 5. Current–voltage characteristic of the stearic acid/calix[4]amine LB film.

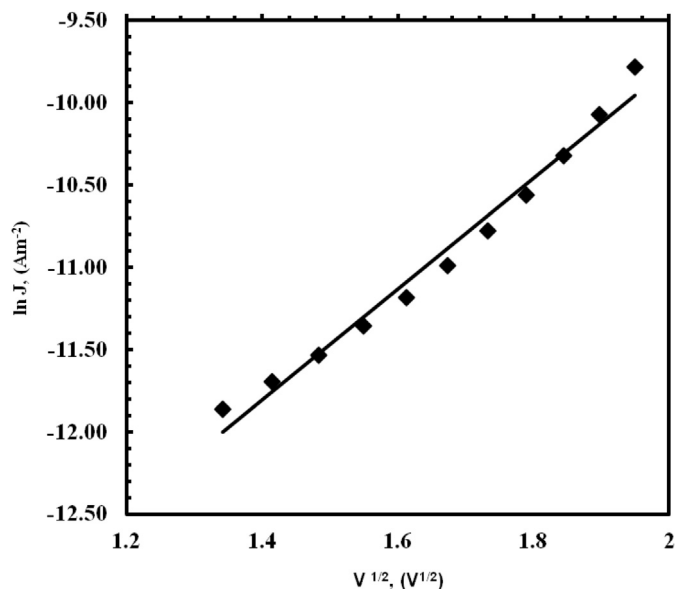


Fig. 6. Plot of $\ln J$ vs $V^{1/2}$ for different voltages.

Using Eq. (9), the experimental value of β for our LB film is calculated as $2.14 \times 10^{-5} \text{ eV m}^{1/2} \text{ V}^{-1/2}$. A theoretical calculation for β using Eq. (8) is made for Poole–Frenkel effect as $4.8 \times 10^{-5} \text{ eV m}^{1/2} \text{ V}^{-1/2}$ and for Schottky effect as $2.4 \times 10^{-5} \text{ eV m}^{1/2} \text{ V}^{-1/2}$. When these values are compared, the experimentally obtained β is more close to the theoretically computed β value for the Schottky effect. According to this result it can be concluded that the conduction mechanism may obey the Schottky effect for carrier transport through the LB film. Further evidence to support such conclusion may be derived from film thickness-independence of measured conductivity, but this information is not available here, however, it has been noted by Geddes and co-workers [21] that possible structural difference in thin films due to different thickness could lead to uncertainties in identifying exact conduction mechanism associated with the $J(V)$ dependence defined by $\ln J \propto V^{1/2}$ relation. This Schottky conduction mechanism is observed for LB films of stearic acid incorporating cadmium ions [30], stearic acid/eicosylamine alternate layer LB film structure incorporating cadmium sulphide CdS nanoparticles [31], non-centrosymmetric Z-type LB films [10] and a calix[4]acid/amine LB thin film [22].

The conduction mechanism is described by Schottky theory and is characterised by Richardson–Schottky law [32]. In Fig. 6 the intercept with the $\ln J$ axis can be expressed in terms of the Schottky barrier height using Eq. (7). The Richardson constant which is described by Richardson–Dushman expression is given as:

$$A = \frac{4\pi m_e e k^2}{h^3} \quad (10)$$

where m_e is the carrier effective mass and it is described by Ref. [33]

$$m_e = \left[\frac{h(e\epsilon_r \epsilon_0)^{1/4}}{1.76\pi^2 kT} \right]^2 E_k^{3/2} \quad (11)$$

$E_k^{3/2}$ is the electric field intensity that corresponds to the transition in conduction mechanism points [21].

To determine the barrier height, Φ_S , of the alternate layer the value of I_0 must be known. This value can be found from the

intercept of current density axis at zero voltage using the graph of $\ln J$ against $V^{1/2}$. ϕ_S is given by:

$$\phi_S = \frac{[kT \ln(\frac{AT^2}{J_0 S})]}{e} \quad (12)$$

Using Eqs. (11) and (12) the carrier effective mass is calculated to be 8.19×10^{-32} kg and ϕ_S value is calculated to be 1.67 eV for the 31 layer stearic acid/calix[4]amine alternate layer LB film.

3.3. AC Measurement analysis

An equivalent circuit model describing the M–LB film–M sandwich device structure is presented in Fig. 2. R_{Metal} is the resistance of the aluminium electrodes, R_{Oxide} and C_{Oxide} are the resistance and capacitance of the aluminium oxide layer between the bottom electrode and the LB film. R_{LB} and C_{LB} are the resistance and capacitance of LB film multilayer.

The AC conductivity, $\sigma(\omega)$, can be described by the following general expression:

$$\sigma(\omega) = \sigma_{\text{dc}}(0) + \sigma_{\text{ac}}(\omega) \quad (13)$$

where σ_{dc} is the dc conductivity at zero-frequency and σ_{ac} is the frequency-dependent component of the conductivity. If the electrode effect is minimized, the insulating LB film sample shows a power law relationship between conductivity and frequency as described below [21]:

$$\sigma_{\text{ac}}(\omega) \propto \omega^s \quad (14)$$

with s value falling in the range between the 0 and 1 and is given by Ref. [34]:

$$s = 1 - \frac{6k_B T}{W_M + k_B T \ln(\omega \tau_0)} \quad (15)$$

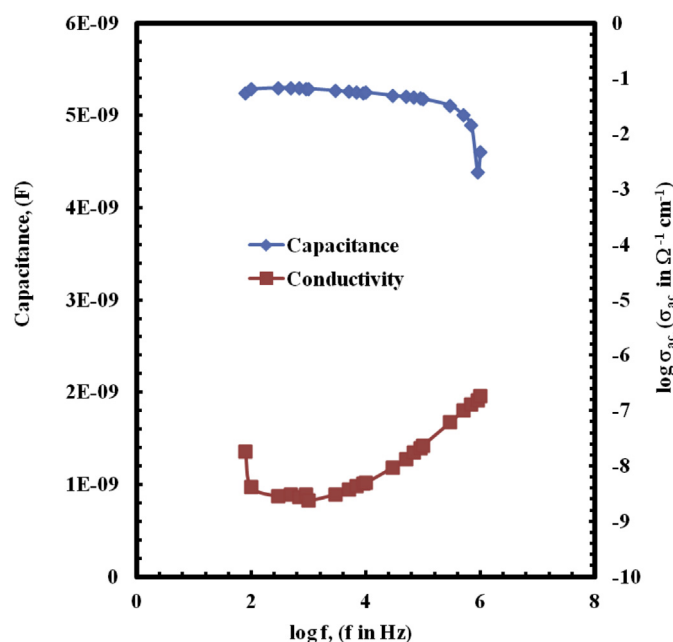


Fig. 7. Dependence of the conductivity and capacitance as a function of $\log f$.

where k_B is the Boltzmann constant, W_M is the effective hopping barrier, T is temperature (22 °C) and τ_0 is the effective relaxation time (10^{-13} s) respectively.

The capacitance and dielectric loss were measured in the frequency range from 80 Hz to 1 MHz at 22 °C. The ac electrical conductivity, σ_{ac} ($\Omega^{-1} \text{ cm}^{-1}$), of the LB film was calculated using the following equation [35,36]:

$$\sigma_{\text{ac}} = \omega \epsilon_0 \epsilon_r \tan \delta \quad (16)$$

where ω is the angular frequency and ϵ_0 is the permittivity of free space. The values of the dielectric constant (ϵ_r) were calculated using Eq. (2). The measured capacitance values (C) and the dielectric loss ($\tan \delta$) of the LB film were recorded directly from the equipment shown in Fig. 4.

Fig. 7 shows the dependence of the ac conductivity as a function of $\log f$. Using the results presented in Fig. 7 for our LB film structure, correlated barrier hopping model is considered to be suitable to describe the experimental data especially for $f > 10$ kHz. The value of $s = 0.81$ at room temperature is calculated using the slope of Fig 7 at 10 kHz. s value for LB films of fatty acid was found to be 0.87 ± 0.02 over the frequency range 10^2 – 10^4 Hz [37]. The value of W_M is found to be 1.30 eV using Eq. (15).

4. Conclusion

Stearic acid/calix[4]amine alternate layer LB films were successfully prepared with a high transfer ratio (~ 0.90) using the LB film deposition procedure to fabricate Metal–LB film–Metal device structures. The pyroelectric characteristics of this LB film structure were determined, the film was found to yield a pyroelectric coefficient of $0.23 \text{ }^\circ\text{C m}^{-2} \text{ K}^{-1}$ and a FOM value of $1.73 \text{ }^\circ\text{C m}^{-2} \text{ K}^{-1}$ at 22 °C. The conduction mechanism within the film was studied using $I(V)$ measurements. These showed a symmetrical and highly non-linear behaviour with an ohmic regime at low voltages, yielding conductivity value of $1.12 \times 10^{-13} \text{ S m}^{-1}$. Within the high voltage region, electron transport obeys the Schottky conduction mechanism. The Schottky potential barrier height for the LB film device obtained from dc measurements was 1.67 eV. These result indicate that the stearic acid/calix[4]amine LB film exhibits behaviour characteristic of an insulator. Using AC measurements the LB films displayed a power law relationship between conductivity and frequency.

[15]

References

- [1] S.A. Hussain, D. Bhattacharjee, *Modern Phys. Lett. B* 23 (2009) 3437–3451.
- [2] A.J. Holden, *IEEE Trans. Ultrason. Ferroelectr. Freq. Control* 58 (2011) 1981–1987.
- [3] A. Hossain, M.H. Rashid, *IEEE Trans. Ind. Appl.* 27 (1991) 824–829.
- [4] A.D. Lantada, P.L. Morgado, H.H. Del Olmo, H. Lorenzo-Yustos, J.E. Otero, J.M. Munoz-Guijosa, J. Munoz-Garcia, J.L.M. Sanz, in: *Biodevices 2009: Proc. Inter. Con. Biomed. Elect. Dev.*, 2009, pp. 453–457.
- [5] V. Norkus, M. Schossig, A. Eydram, G. Gerlach, in: F. Berghmans, A.G. Mignani, P. Demoor (Eds.), *Optical Sensing and Detection II*, Book Series: Proceedings of SPIE, vol. 8439, 2012, p. 84391.
- [6] B. Tesneli, A. Topacli, C. Topacli, M. Durmus, V. Ahsen, *Colloids Surf. A* 299 (2007) 247–251.
- [7] R. Çapan, *Mater. Lett.* 61 (2007) 1231–1234.
- [8] S. Ma, S. Li, W. Wang, G. Wang, J. Sun, X. Meng, J. Chu, *Colloids Surf. A* 284/285 (2006) 74–77.
- [9] F. Aouni, A. Rouis, H.B. Ouada, R. Mlika, C. Dridi, R. Lamartine, *Mater. Sci. Eng. C* 24 (2004) 491–495.
- [10] R. Çapan, A.K. Ray, T.H. Richardson, A.K. Hassan, F. Davis, *J. Nanosci. Nanotechnology* 5 (2005) 1910–1914.
- [11] R. Çapan, I. Alp, T.H. Richardson, F. Davis, *Mater. Lett.* 59 (2005) 1945–1948.
- [12] D. Lacey, T. Richardson, F. Davis, R. Çapan, *Mater. Sci. Eng. C* 8/9 (1999) 377–384.
- [13] C.M. McCartney, T. Richardson, M.A. Pavier, F. Davis, C.J.M. Stirling, *Thin Solid Films* 327/329 (1998) 431–434.

- [14] T. Richardson, M.B. Greenwood, *Langmuir* 11 (1995) 4623–4625.
- [15] T. Richardson, M.B. Greenwood, F. Davis, C.J.M. Stirling, *IEEE Proc. Circuits Dev. Syst.* 144 (1997) 108–110.
- [16] P. Oliviere, J. Yarwood, T.H. Richardson, *Langmuir* 19 (2003) 63–71.
- [17] W.H. Abd. Majid, T.H. Richardson, D. Lacey, A. Topaçli, *Thin Solid Films* 376 (2000) 225–231.
- [18] R. Capan, I. Basaran, T.H. Richardson, D. Lacey, *Mater. Sci. Eng. C* 22 (2002) 245–249.
- [19] T.H. Richardson, *Functional Organic and Polymeric Materials*, Wiley, England, 2000.
- [20] A.V. Nabok, B. Iwantono, A.K. Hassan, A.K. Ray, T. Wilkop, *Mater. Sci. Eng. C* 22 (2002) 355–358.
- [21] N.J. Geddes, J.R. Sambies, W.G. Parker, N.R. Couch, D.J. Jarvis, *J. Phys. D Appl. Phys.* 23 (1990) 95–102.
- [22] R. Capan, F. Davis, *Mater. Chem. Phys.* 125 (2011) 883–886.
- [23] I. Çapan, T. Uzunoglu, Ç. Tarımcı, T. Tandırsever, *Thin Solid Films* 516 (2008) 8975–8978.
- [24] K. Kobayashi, Y. Tomita, K. Matsuhisa, Y. Doi, *Appl. Surf. Sci.* 244 (2005) 389–393.
- [25] J.G. Simmons, *Phys. Rev.* 155 (1967) 657–660.
- [26] L.J. Anderson, M.V. Jacob, *Mater. Sci. Eng. B* 177 (2012) 311–315.
- [27] N. Nagaraj, C.V.S. Reddy, A.K. Sharma, V.V.R.N. Rao, *J. Power Sources* 112 (2002) 326–330.
- [28] R.D. Gould, T.S. Shafai, *Thin Solid Films* 373 (2000) 89–93.
- [29] R.D. Gould, B.B. Ismail, *Vacuum* 50 (1998) 99–101.
- [30] T. Uzunoglu, R. Capan, H. Sari, *Mater. Chem. Phys.* 117 (2009) 281–283.
- [31] R. Çapan, A.K. Ray, A.K. Hassan, *Thin Solid Films* 515 (2007) 3956–3961.
- [32] M.D. Stamate, *Appl. Surf. Sci.* 205 (2003) 353–357.
- [33] M. Rusu, G.I. Rusu, *Appl. Surf. Sci.* 126 (1998) 246–254.
- [34] A.A. Dakhel, *Chem. Phys. Lett.* 393 (2004) 528–534.
- [35] M.A.F. Basha, R.M.M. Morsi, *J. Non-Cryst. Solids* 357 (2011) 1056–1062.
- [36] R.M.M. Morsi, M.A.F. Basha, *Mater. Chem. Phys.* 129 (2011) 1233–1239.
- [37] M. Sugi, K. Nembac, D. Möbius, H. Kuhn, *Solid State Commun.* 13 (1973) 603–606.